

# Wide Bandwidth, High Performance Waveguide-Integrated P-I-N Photodiodes For 40 Gbits/s Receiver Modules

G. Wang, M. Takechi, K. Araki, T. Tokumitsu, I. Hanawa, Y. Yoneda, K. Sato and M. Kobayashi

Fujitsu Quantum Devices Limited, 1000 Kamisukiahara, showa-cho, Nakagoma-gun, Yamanashi 409-3883, Japan

6:

**Abstract** — A side-illuminated waveguide integrated PIN photodiodes (WG PIN PD) has been developed and modeled for use in 40 Gb/s PIN/PREAMP receiver module. The WG PIN PD exhibited a wide bandwidth over 40 GHz with a high responsivity. For the PIN/PREAMP modules with a GaAs pHEMT traveling wave amplifier (TWA), a clear eye-opening was observed and a recorded minimum received power of -11.2 dBm at 40 Gb/s was obtained for the first time.

## I. INTRODUCTION

Optical receiver modules for the next-generation 40 Gbits/s optical-fiber communication systems create a strong demand for very fast and high reliability photodiodes (PDs). To overcome the bandwidth-efficiency tradeoff in the conventional vertically illuminated PDs, the edge-coupled PDs have received a great deal of interest [1]. Usually, in this structure, an optical waveguide structure is also integrated in itself to obtain efficient optical coupling [2]. Thus, for the edge-coupled PDs, the optical absorption depth and the carrier transit length are decoupled, a very large bandwidth-efficiency product can be realized [3]. In addition, a large bandwidth-efficiency product is an essential factor for bring out the full potential of a receiver.

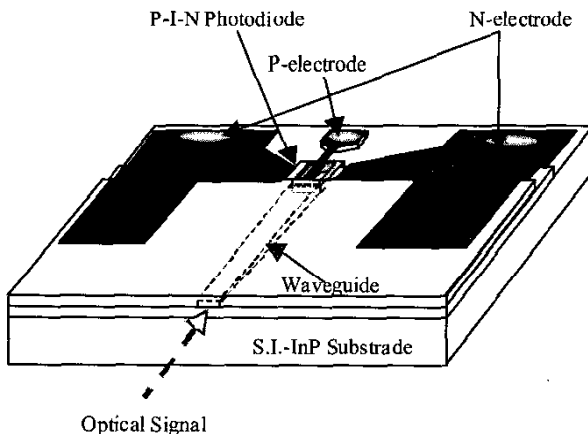


Fig. 1 Schematic view of a WG PIN PD.

In this paper, we report the design and technology of a tapered thickness waveguide integrated side-illuminated P-I-N photodiode (WG PIN PD). A small-signal equivalent circuit model that includes both external parasitic elements and intrinsic opto-electronic conversion performance is proposed to analysis the  $S$ -parameters of high speed P-I-N photodiodes. The WG PIN PD simultaneously exhibited a wide bandwidth over 40 GHz and a high typical external responsivity over 0.85 A/W. By using the WG PIN PD and a GaAs pHEMT traveling wave amplifiers, a record high PIN/Preamp receiver sensitivity -11.2 dBm has been achicved. A close agreement between simulated and measured frequency response was also confirmed.

## II. DEVICE STRUCTURE OF WG PIN PD

Figure 1 shows the schematic structure of the side-illuminated  $p^+$ -InP/i-InGaAs/n-InP waveguide-integrated double-hetero junction WG PIN PD. The waveguide of this PD functions as a spot-size converter in which the thickness of an InGaAsP core tapers in the propagation direction. The waveguide was fabricated by using selective MOCVD growth technology. The P-I-N junction area is  $6 \mu\text{m} \times 7 \mu\text{m}$  and the thickness of InGaAs optical absorption layer is  $0.28 \mu\text{m}$ . The P-I-N junction area is buried in semi-insulating InP. To reduce the parasitic capacitance, the bonding pad of p-electrode was fabricated on the semi-insulating InP substrate, and the P-I-N junction area and the bonding pad are connected by an air-bridge wire. An anti-reflective coating was also formed on the cleaved optical input facet of the WG PIN PD.

## III. SMALL SIGNAL S-PARAMETER MODEL OF WG PIN PD

Frequency-domain optical responses ( $S_{21}$ ) and the reflection coefficients ( $S_{22}$ ) of the studied WG P-I-N PD were measured by a 50-GHz lightwave component analyzer equipment (HP/Agilent 8603A). The laser with a 1550-nm center wavelength was used as the measurement

source. The device was contacted by a  $50 \Omega$  GSG microwave probe.

Fig. 2 (a) shows the measured  $S_{22}$  versus frequency (from 45 MHz to 50 GHz) of the WG PIN PD structure on Smith chart. Fig. 2 (b) shows the small signal frequency characteristics of the WG PIN PD ( $S_{21}$ : noised line) measured at  $-5$  V bias voltage and below 10 mW optical input power. The 3-dB bandwidth  $f_{3-\text{dB}}$  is estimated to be over 40 GHz.

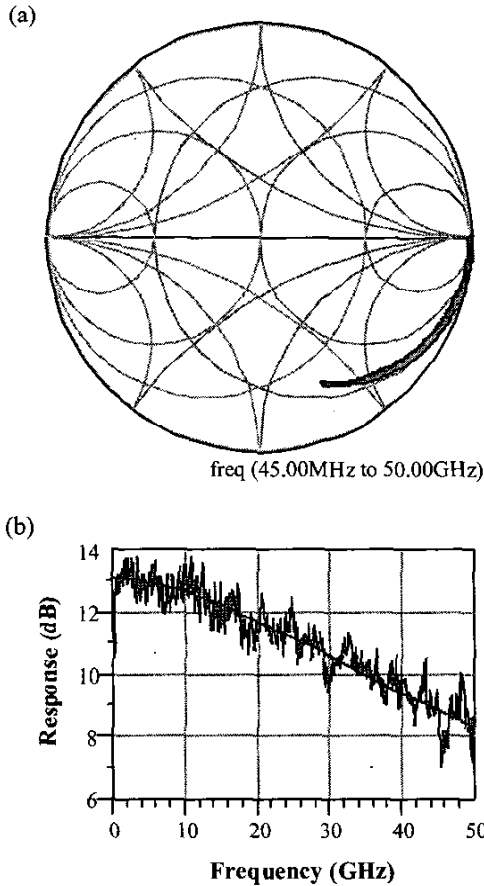


Fig. 2 (a) Measured and calculated  $S_{22}$  (normalized to  $50 \Omega$ ) versus frequency of the WG PIN PD on Smith Chart. (b) Frequency response characteristic ( $S_{21}$ ) for the WG PIN PD measured at 5 mW optical input power and  $-5$  V bias.

In order to obtain small-signal equivalent-circuit element values from the measured  $S$ -parameters, a small-signal RF equivalent circuit involving the parasitic elements of the WG PIN PD is modeled [4] and shown in Fig. 3 (a), where  $R_c$  is the p-electrode contact resistance;  $R_s$  is the resistance of  $\text{P}^+$ -InP layer;  $C_j$  is the reverse bias junction capacitance;  $C_{\text{dx}}$  is the capacitance between the

air-bridge and n-electrode pad;  $C_p$  is the p-electrode pad capacitance;  $L_s$  is the inductance of the air-bridge from p-contact to p-electrode pad. Extraction of the parasitic values in the small-signal equivalent circuit were carried out by best-fitting the measured  $S_{22}$  parameter (Fig. 2 (a)), and the extracted values for the WG P-I-N PD at  $-5$  V bias voltage are also given in Fig. 3 (a). The photocurrent source  $i(\omega)$  due to optical input was modeled as shown in Fig. 3 (b), in which the ac photocurrent  $i(\omega)$  that flows out to the external parasitic circuit was controlled by the delayed voltage  $e_o(\omega)$  across the  $R_t C_t$  circuit equivalent to carrier drift-induced time delay. The current source is represented as  $i(\omega) = g_m e_o(\omega)$ , where  $g_m e_o(0)$  represents the DC level and is adjusted to the optical conversion quantum efficiency. The parallel circuit element  $C_{\text{sc}}$  is applied to equivalently represent the stored charge effect that instantaneously modulate the depletion capacitance and yield a further nonlinear effect for very large input power and output current level. The equivalent circuit model shown in Fig. 3 (b) determines the intrinsic opto-electronic conversion performance.

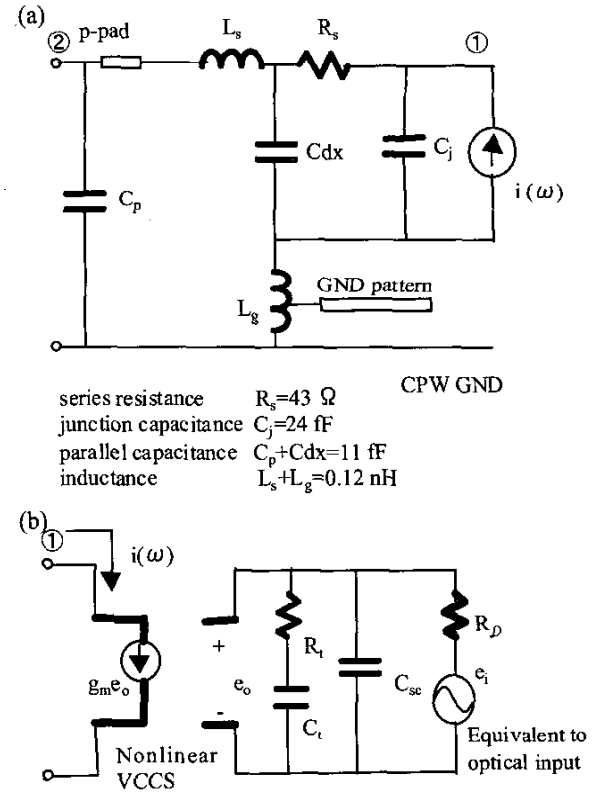


Fig. 3 Small signal equivalent circuit of WG PIN PD: (a) equivalent circuit that only involves the parasitic elements and (b) model of photo current source that determines the intrinsic opto-electronic conversion performance.

By combining the models for the external and intrinsic equivalent circuit shown in figures 3 (a) and (b), the  $S_{21}$  characteristics of the studied WG PIN PD was completely modeled even for a very large optical input levels. As shown in Fig. 2 (b), the simulated  $S_{21}$  curve (solid line) can be best-fitted with the measured  $S_{21}$  curve (noised line) by carefully choosing the external and intrinsic equivalent circuit elements in Fig. 3.

In addition, it can be seen that the wide bandwidth of the WG PIN PD was obtained due to the low parasitic capacitance, series resistance and the optimized design of the device structure.

#### IV. PIN/PREAMP RECEIVER SENSITIVITY OF THE WG PIN PD

The PIN/PREAMP receiver module was designed focusing on not only performance but also mass productivity and reliability. A GaAs pHEMT traveling wave amplifier (TWA), which has the bandwidth greater than 45 GHz and the typical transimpedance of 150  $\Omega$ , was used as the transimpedance amplifier (TIA) with the WG PIN PD. The schematic structure of the receiver module is shown in Fig. 4.

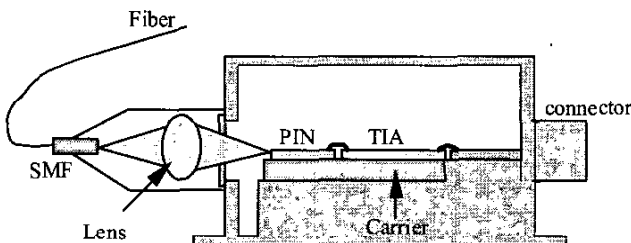


Fig. 4 Schematic structure of the PIN/PREAMP receiver module.

The frequency response of the receiver module was measured by the lightwave component analyzer from 45 MHz to 50 GHz. As shown in Fig. 5, the typical measured 3dB bandwidth is 45 GHz. Basing on the newly proposed small-signal equivalent circuit model of the WG PIN PD in Fig. 3, the PIN/PREAMP receiver module is modeled and the overall frequency properties is simulated. The simulated frequency response of the receiver module is also shown in Fig. 5. The measured  $S_{21}$  parameter of the GaAs pHEMT preamplifier is used in the simulation process. It can be seen that the simulated frequency response give a very good description of the measured one from 45 MHz to 50 GHz. This proves that this approach provides a method that directly predicts and analyzes the frequency response properties of ultra fast PIN/PREAMP receiver module using a full electrical equivalent circuit.

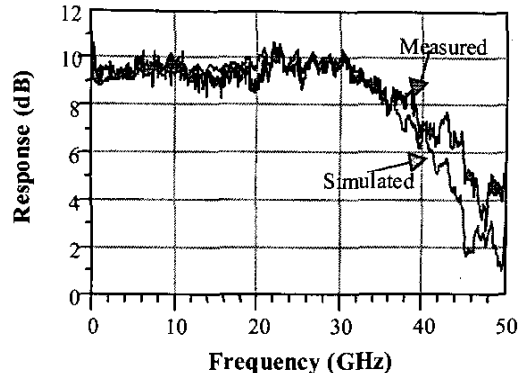


Fig. 5 The measured and the simulated frequency response characteristic for the PIN/PREAMP receiver module.

Non-return-to-zero (NRZ) eye-pattern at 40 Gb/s and  $2^{31}-1$  pseudo random binary sequence (PRBS) was measured using the in-house optical transmitter. Agilent 86100A digital communication analyzer with 86107A precision time base module and 86116A module, which has 65 GHz electrical bandwidth, was used for waveform monitoring. The NRZ eye-pattern at 0 dBm average optical input power is shown in Fig. 6. Large eye opening and low gitter indicate that the receiver module has a good amplitude and phase linearity over the receiver bandwidth.

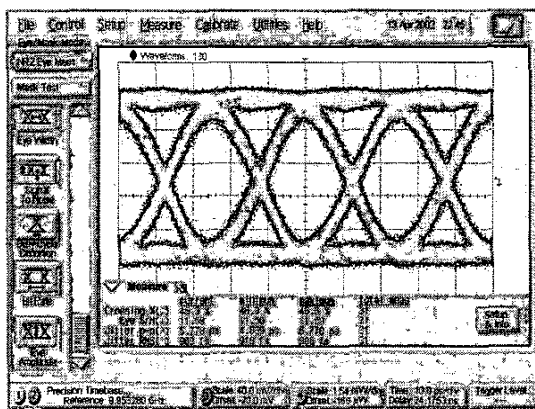


Fig. 6 40Gb/s NRZ eye patterns at 0 dBm average optical input power.

40 Gb/s NRZ bit error rate (BER) performances of receiver were measured using the same system used in the eye-pattern evaluation. Due to inferior low-frequency characteristics of measurement system,  $2^7-1$  PRBS signal was used in the BER measurement instead of  $2^{23}-1$  PRBS signal. The postamplifier, which have 20 dB gain and 27 GHz bandwidth, was connected between the output of the

receiver module and the error analyzer to feed sufficient voltage swing to the error analyzer. The extinction ratio of optical signal was about 10. Fig. 7 shows the back-to-back BER characteristics. The minimum received power was as low as -11.2 dBm at a BER of  $10^{-9}$ . This is, to our knowledge, the highest 40 Gb/s PIN/PREAMP receiver sensitivity so far reported not employing fiber pre-amplifier. It is expected that a better receiver sensitivity will be achieved by improvement of the BER measurement system and increasing of post-amplifier bandwidth.

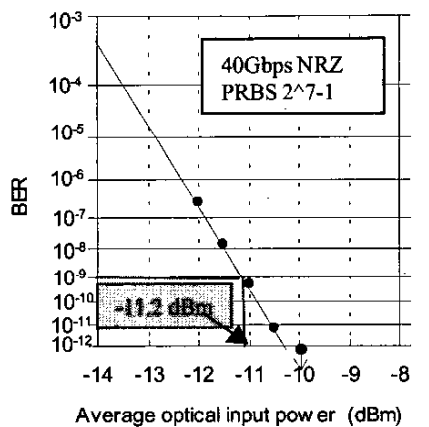


Fig. 7 Back-to-back PIN/PREAMP receiver sensitivity for WG PIN PD at 40 Gb/s NRZ.

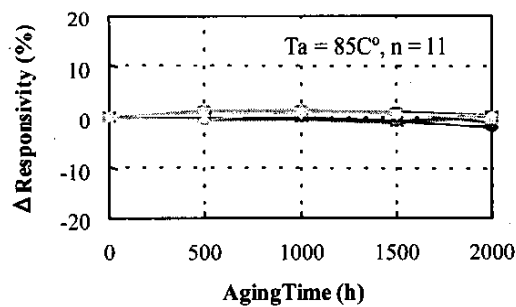


Fig. 8 Variation of responsivity by high temperature storage.

To investigate the reliability of the optical coupling of the PIN/PREAMP receiver module, temperature storage test was conducted. Fig. 8 shows the result of aging test up to 2000 hours at 85°C. It can be seen no noticeable degradation of responsivity was observed. This proved the optical coupling system of our modules was robust and reliable.

## V. CONCLUSION

In summary, a high performance, high reliability side-illuminated tapered waveguide integrated PIN photodiode (WG PIN PD) was developed for use in 40 Gb/s receiver modules. The WG PIN PD has a wide bandwidth of more than 40 GHz due to the low parasitic capacitance and resistance. High reliability of WG PIN PD was confirmed up to 5000 hours by a aging test at 175°C and bias-voltage of 10 V. For the PIN/PREAMP modules with a GaAs pHEMT TWA, a recorded minimum received power of -11.2 dBm at 40 Gb/s was obtained. We believe that the WG PIN PD and PIN/PREAMP receiver module will be very suitable in 40 Gb/s optical communications systems.

## ACKNOWLEDGEMENT

The authors would like to thank Y. Furukawa and T. Kawano of FQD for module design and assembly, B. Truong of FCSI for helps in module measurement.

## REFERENCES

- [1] K. Kato, S. Hata, K. Kawano and A. Kozen, "Design of ultrawide-band, high-sensitivity p-I-n photodetectors", IEICE Trans. Electron, Vol. E76-C, pp. 214-221, 1993.
- [2] K. Kato, "Ultrawide-band/high-frequency photodetectors" IEEE Trans. Microwave Theory Tech., Vol. 47, pp. 1265-1280, 1999.
- [3] N. Yasuoka, M. Makiuchi, M. Miyata, O. Aoki, M. Egawa, N. Okazaki, M. Takechi, H. Kuwatsuka and H. Soda, "High-efficiency PIN photodiodes with a spot-size converter for 40 Gb/s transmission systems", Proc. ECOC2001, Sept. 30-Oct. 4, pp.558-559, 2001.
- [4] G. Wang, T. Tokumitsu, I. Hanawa, K. Sato and M. Kobayashi, "Analysis of High Speed P-I-N Photodiodes S-parameters By a Novel Small-Signal Equivalent Circuit Model", IEEE Microwave and Wireless Components Letters, Vol. 12, No. 10, OCTOBER 2002.